# The impacts of pollution sources and temperature on the light absorption of HULIS were revealed by UHPLC-HRMS/MS at the molecular structure level

*Tao Qiu[a], Yanting Qiu[b], Yongyi Yuan[a], Rui Su[c], Xiangxinyue Meng[b], Jialiang Ma[d], Xiaofan Wang[b], Yu Gu[a], Zhijun Wu[b,]*, Yang Ning[a], Xiuyi Hua[a], Dapeng Liang[a,]*, Deming Dong[a]*

[a] Key Lab of Groundwater Resources and Environment of the Ministry of Education, College of New Energy and Environment, Jilin University, Changchun 130012, China

[b] State Key Laboratory of Regional Environment and Sustainability~~State Key Laboratory of Environmental Systems and Security~~, College of Environmental Sciences and Engineering, Peking University, Beijing 100871, China

[c] State Key Laboratory of Inorganic Synthesis and Preparative Chemistry, College of Chemistry, Jilin University, Changchun 130012, China

[d] Department of Chemistry, Aarhus University, 8000 Aarhus C, Denmark

*Corresponding Author: Dapeng Liang (liangdp@jlu.edu.cn) and Zhijun Wu (zhijunwu@pku.edu.cn)

**ABSTRACT.** Atmospheric humic-like substances (HULIS), a key component of brown carbon (BrC), significantly promote the light absorption of aerosols. However, their linkages to pollution sources and ambient temperature in cold environments remain unresolved. Here, we analyze wintertime urban aerosol samples in Changchun, Northeast China, using ultrahigh performance liquid chromatography coupled with high-resolution tandem mass spectrometry (UHPLC-HRMS/MS). HULIS show a high light absorption efficiency ($MAE_{365}$ = 1.81 ± 0.24 $m^2$ $gC^{-1}$) and high mass concentration (2.97 ± 1.54 $\mu$gC $m^{-3}$), exceeding values reported from other global regions. Through UHPLC-HRMS/MS characterization, we identify 264 compounds at the molecular structure level, accounting for 38.2 - 78.1% of the total HULIS mass. Compositional analysis demonstrates biomass burning and coal combustion are the main BrC sources during haze events. We screen out 39 strong BrC chromophores, mainly nitrophenols, that contribute 28.9 ± 10.4% of the total light absorbance at 365 nm. Low ambient temperatures potentially enhance the accumulation of these strong BrC chromophores in the aerosol particles by suppressing photobleaching processes and altering thermodynamic reaction equilibria. These findings emphasize the potential of BrC to exert a more significant and persistent environmental effect in the cold region atmosphere.

**KEYWORDS:** *Humic-Like Substances, Non-targeted screening, Northeast China, Light absorption efficiency, Brown carbon chromophores.*

## Graphical Abstract

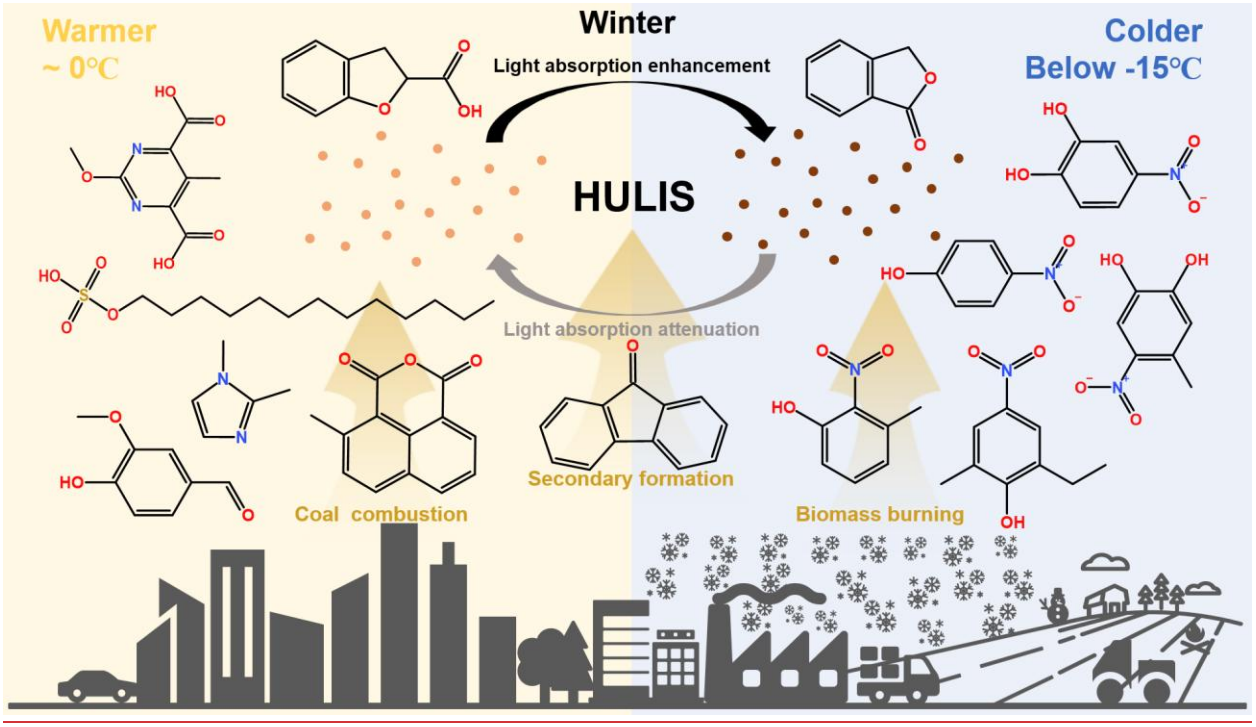


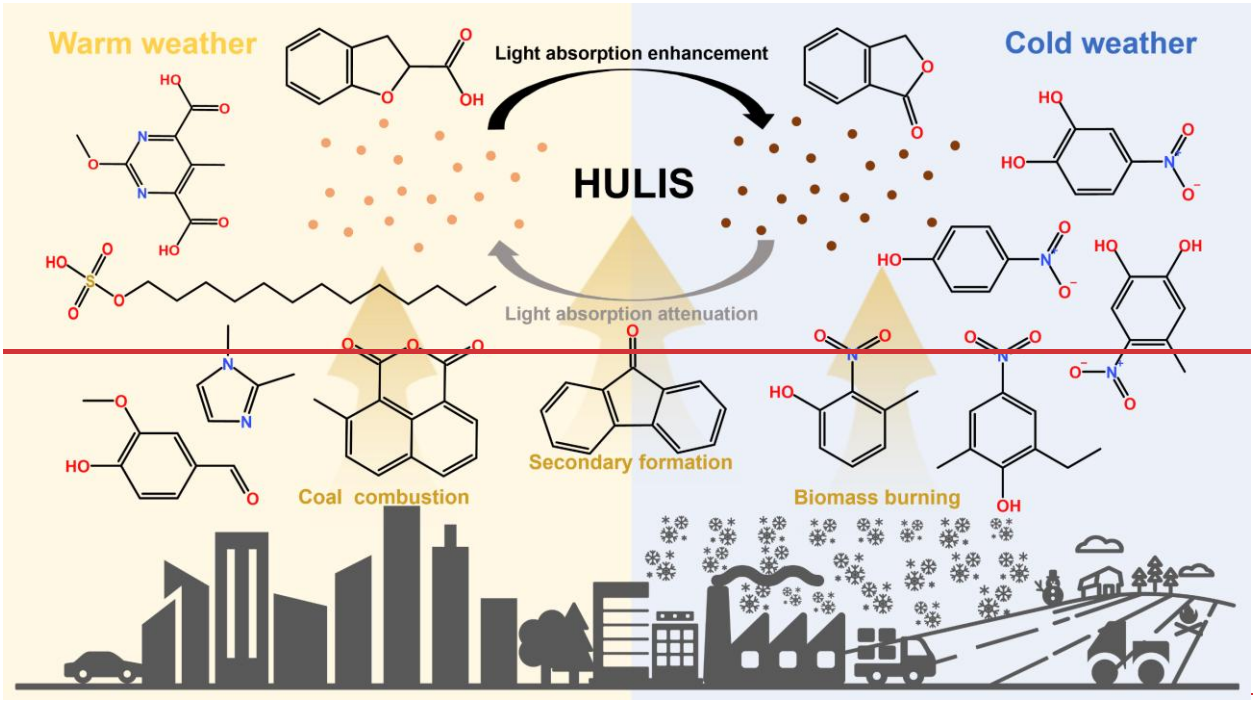

## 1. Introduction

Atmospheric humic-like substances (HULIS) are important components in light-absorbing aerosols (Hoffer et al., 2006; Zou et al., 2023), therefore affecting global radiative forcing and atmospheric chemical processes (Chung et al., 2012; Huang et al., 2020; Laskin et al., 2015). They are identified as a highly complex aggregate of polar organic compounds composed of aromatic, aliphatic, and alicyclic structures with functional groups such as hydroxy, carbonyl, carboxyl, nitrooxy, and sulfooxy (Song et al., 2018; Wang et al., 2019; Zou et al., 2023). Previous studies have revealed that the molecular composition of HULIS determine their physicochemical properties, further impacting their climatic and environmental effects, such as cloud condensation nuclei activation, human health, and global radiation (Bao et al., 2023; Cappiello et al., 2003; Chen et al., 2021; Dou et al., 2015; Hems and Abbatt, 2018; Krivácsy et al., 2000).

As reactive components in the atmosphere, HULIS exhibit pronounced chemical activity through their oxygenated functional groups, particularly prone to the oxidation by reactive oxygen radicals and gaseous oxidants (Hems et al., 2021; Huo et al., 2021; Qiu et al., 2024). Both laboratory simulations and field observations have demonstrated that these atmospheric aging processes significantly alter the light-absorption ~~features~~ properties and environmental behaviors of HULIS (Hems and Abbatt, 2018; Qiu et al., 2024; Wang et al., 2022, 2019). Furthermore, significant efforts have been directed towards understanding the link between molecular composition and light absorption of HULIS. Studies have suggested that chromophores like nitroaromatics and oxygenated polycyclic aromatics are key contributors to the light absorption of HULIS (Kuang et al., 2023; Qin et al., 2022; Song et al., 2019; Zou et al., 2023). However, critical knowledge gaps persist regarding the molecular structures that dominate light absorption and, importantly how these molecules and their associated absorption properties evolve during atmospheric aging processes. ~~Although extensive investigations have characterized the elemental composition of HULIS , critical knowledge gaps persist regarding the molecular structures determining their light absorption.~~ This limits comprehension understanding of the atmospheric evolution process and radiative effect of HULIS.

~~Following~~ Once emit~~ssions~~ into or form in the atmosphere, ~~HULIS undergo~~ vertical transport increased the altitude of HULIS-containing particles, leading to long-range transport~~accompanied by sharp ambient temperature declines~~ (Chen et al., 2021; Slade et al., 2017). During vertical transportation, the ambient temperature sharply decreases, indicating that the atmospheric evolution of HULIS accompanies with low-temperature conditions during their majority lifetime~~This indicates that the atmospheric evolution of HULIS is under low temperature conditions during their majority lifetime~~ (Heald et al., 2005; Liu et al., 2014; Pani et al., 2022; Textor et al., 2006; Wu et al., 2018a). How low temperature impacts the atmospheric evolution process of HULIS remains uncertain yet. The decrease in temperature could potentially alter the physicochemical properties of HULIS, influencing their volatility (Cao et al., 2018; Schervish and Donahue, 2020), reactivity (Liu et al., 2023; Slade et al., 2017), and partitioning between the gas and particulate phase (Arp et al., 2008; Tao and Murphy, 2021). Consequently, their light absorption and atmospheric lifetime ~~might be~~are profoundly affected (Gregson et al., 2023; Roelofs, 2013). Therefore, it is imperative to further explore the low-temperature behavior of HULIS through field observations in cold environments.

This study collected atmospheric $PM_{2.5}$ samples in Changchun, which experiences low temperatures in wintertime, and HULIS were subsequently extracted. By employing a combination of non-targeted analysis and ultrahigh performance liquid chromatography coupled with high-resolution tandem mass spectrometry (UHPLC-HRMS/MS), we aimed to identify the molecular structures in HULIS collected from urban aerosols during wintertime.

This approach provided us new insights into the potential sources and temperature effects on the light-absorption properties of HULIS.

## 2. Experimental Section

**2.1 Aerosol sampling and HULIS extraction.** We conducted a field campaign on the campus of Jilin University in Changchun, Northeast China (125.29° E, 43.83° N) from January 1st to 30th, 2023. During this period, a high-volume particulate sampler (Tianhong Intelligent Instrument Plant, Wuhan, China, 1.05 $m^3$ $min^{-1}$) collected 24 h $PM_{2.5}$ samples on a pre-baked quartz filter. **Figure S5** presented the meteorological data (http://www.wunderground.com/) and air pollutants data (http://air.cnemc.cn:18007/), including relative humidity, temperature, concentrations of CO, $SO_2$, $O_3$, $NO_2$, $PM_{2.5}$, and $PM_{10}$ during the sampling campaign.

The preparation process of HULIS sample was identical with previous studies (Limbeck et al., 2005; Yuan et al., 2021; Zou et al., 2020), and can be briefly described as the following steps: sampled filter was firstly extracted with ultrapure water (> 18.2 MΩ) in an ultrasonic bath for 40 mins. After that, the water extracts were filtered through 0.22 $\mu$m PES syringe filters, then acidified to pH=2 by HCl solution (0.1 M) and loaded on the pre-acidification solid phase extraction (SPE) cartridges (Supelclean ENVI-18, 500 mg, 3 mL). The majority of inorganic ions, low molecular-weight organic acids, and sugars were eluted out with ultrapure water while the fractions retained in the SPE cartridge were eluted with methanol (Baduel et al., 2009). Finally, a portion of the elution was measured by UHPLC-HRMS/MS and the rest was dried under a gentle stream of $N_2$, then redissolved in ultrapure water for total organic carbon and light absorption analysis.

**2.2 Molecular composition analysis of HULIS.** An ultrahigh performance liquid chromatography system (UHPLC, Dionex Ultimate 3000, Thermo Fisher Scientific, San Jose, CA, U.S.A.) coupled with an Orbitrap Fusion Tribrid mass spectrometer (Thermo Fisher Scientific, San Jose, CA, U.S.A.) was used to detect the molecular composition of HULIS. To detect as many HULIS species as possible and achieve quantification, we optimized the detection method (detailed in **Text S1**) to decrease the method detection limit and applied a semi-quantitative strategy to quantify the identified compounds.

The optimized chromatographic conditions were as follows: Accucore C18 2.6 $\mu$m particle size (100 × 2.1 mm, Thermo Scientific) with the gradient elution started from 80% of mobile phase A (0.05% acetic acid) with a 0.2 mL $min^{-1}$ flow rate for 2 min, then changed to 100% of mobile phase B (methanol with 0.05% acetic acid) in 15 min and maintained constant for 2 min, decreased to 20% of mobile phase B within 1 min and finally held for 3 min for re-equilibration. The mass spectra (*m/z* 60-600) with a resolving power of 120,000 (*m/z* 200) were obtained by using heated-electrospray ionization (H-ESI). The optimized mass spectrometric parameters were as follows: 3.5 kV spray voltage for positive ions and 3.25 kV spray voltage for negative ions, 35 psi sheath gas (nitrogen), and 10 psi auxiliary gas (nitrogen), 320 °C ion transfer tube temperature, 125 °C vaporizer temperature. The data acquisition used data dependent mode and the master scans interval time was set as 1.0 second for the full scan experiments (detailed in **Table S5**).

The obtained data analysis was performed with the Compound Discoverer 3.3 software to generate reasonable molecular formulas and match fine structures to MS/MS data. The numbers of atoms restriction of formula were 1-40 for C, 1-100 for H, 0-40 for O, 0-6 for N, and 0-2 for S, with $0.3 \leq H/C \leq 3.0$, $0 \leq O/C \leq 1.2$,

$0 \leq N/C \leq 1.0$, and $0 \leq S/C \leq 0.8$ (Kind and Fiehn, 2007). All of the mathematically formulas for each peak were performed with a mass tolerance of ± 5 ppm and peak areas more than three times of the blank sample. Three curated spectral databases, mzcloud library database, ChemSpider library database, and CFM-ID (https://cfmid.wishartlab.com) were applied to screen suspect candidates of structure (Allen et al., 2015). According to the Schymanski's confidence level (CL), these candidates were divided into confirmed structures (CL1), probable structures (CL2), and tentative candidates (CL3) (Schymanski et al., 2014). We showed two examples to illustrate the derivation processes of candidates in **Figure S6**.

A semi-quantitative strategy was conducted as follows: target analytes were quantified using external standard solutions of structurally analogous surrogate compounds (Nguyen et al., 2014; Nozière et al., 2015). A representative application involved utilizing the standard curve of 4-methyl-5-nitrocatechol to simultaneously quantify three structural analogs: 4-methyl-5-nitrocatechol, 3-methyl-5-nitrocatechol, and 3,4-dimethyl-5-nitrocatechol. While this strategy enables quantification of compounds without commercially available standards, it introduces inherent uncertainties due to ionization efficiency variations between surrogates and target analytes (discussed in **Text S2**).

**2.3 Light absorption analysis of HULIS and other analysis.** A total of the HULIS extract was first diluted to 3 mL with ultrapure water and then measured by a UV-Vis spectrophotometer (UV-1900, Shimadzu, Kyoto, Japan) at 200-700 nm with an interval wavelength of 1 nm. To assess the optical properties of HULIS samples, the mass absorption efficiency ($MAE_\lambda$ , $m^2\ gC^{-1}$) was calculated according to the following formula.

$$Abs_\lambda = (A_\lambda - A_{700})\frac{V_l}{V_a \times l}\ln 10 \qquad (1)$$

$$MAE_\lambda = \frac{Abs_\lambda}{C} \qquad (2)$$

where $Abs_\lambda$ represents the light absorption coefficient of the HULIS extract at a wavelength of $\lambda$ nm ($Mm^{-1}$), $A_\lambda$ is the recorded absorbance value of the HULIS extract by the UV-Vis spectrophotometer, $V_l$ is the total solution volume of HULIS extract (mL), $V_a$ is the air sampling volume corresponding to the volume of HULIS extract ($m^3$), $l$ represents the optical path length (0.01 m), $C$ is the mass concentration of HULIS carbon (HULIS-C) ($\mu gC\ m^{-3}$).

The contents of elemental carbon (EC) and organic carbon (OC) in quartz fiber filters were determined by a Thermo-Optical Transmission (TOT) method on a Sunset Lab EC/OC analyzer. The concentrations of HULIS-C were analyzed by a total organic carbon (TOC) analysis (TOC-L, Shimadzu, Kyoto, Japan). Additionally, the ratio of OC emitted from combustion to TOC was calculated by the assigned formula (Cabada et al., 2004).

$$OC_{com}/OC_{total} = (\left[\frac{OC}{EC}\right]_p * [EC])/[OC] \qquad (3)$$

where $OC_{com}/OC_{total}$ represents the ratio of OC emitted from combustion to total OC, $[OC/EC]_p$ is the ratio of OC to EC for the primary sources, $[EC]$ and $[OC]$ are the measured EC and OC concentration, respectively.

~~The w~~Water-soluble inorganic ions in $PM_{2.5}$ collected on Teflon filter were detected by ion chromatography (IC, Shimadzu, Kyoto, Japan). The aerosol liquid water content (ALWC) and pH were calculated using the ~~ISORROPIA~~ ISORROPIA-II thermodynamic model based on meteorological data and mass concentrations of water-soluble

inorganic ions (Fountoukis and Nenes, 2007; Nenes et al., 1998; Wu et al., 2018b).

## 3. Results and Discussion

**3.1 Molecular composition and light absorption of HULIS. Figure 1A** illustrated the temporal variations of HULIS-C, OC, and EC mass concentrations ~~over~~ during the ~~entire~~ sampling period. The~~during which~~ temperatures ranged from 2.9 to -25.3 ℃ and solar radiation ranged from 24.3 to 57.8 W $m^{-2}$ (**Figure 1B**). The average concentrations of OC and EC were 11.7 ± 5.74 and 2.06 ± 0.92 $\mu$g $m^{-3}$, respectively. The average HULIS-C concentration was~~amounted to~~ 2.97 ± 1.54 $\mu$g $m^{-3}$, accounting for~~constituting~~ 25.1% of ~~the~~ total OC. The observed HULIS-C concentration ~~exceeded levels documented~~was higher than those observed in winter of Europe (0.68 – 1.47 $\mu$g $m^{-3}$) (Emmenegger et al., 2007; Voliotis et al., 2017), South America (0.2068 – 1.3047 $\mu$g $m^{-3}$) (Serafeim et al., 2023), and Chinese other regions (1.96 – 2.38 $\mu$g $m^{-3}$) (Lu et al., 2019; Ma et al., 2019; Zou et al., 2023), indicating the abundance of HULIS in Changchun.

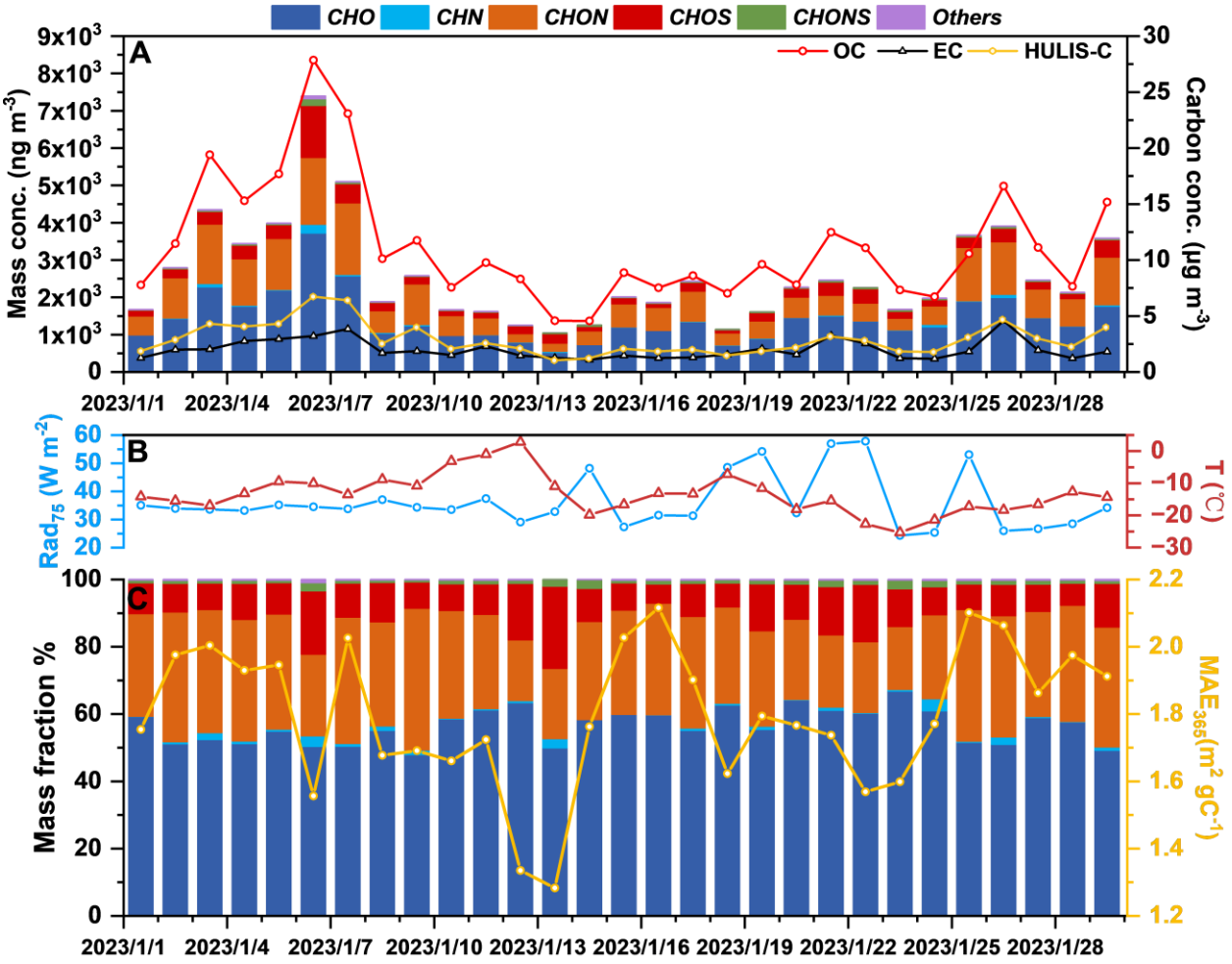


**Figure 1.** Temporal variations in the mass concentrations of six compound categories, organic carbon, and elemental carbon (A); the 75$^{th}$ percentile of solar radiation ($Rad_{75}$) and ambient temperature (B); the mass fraction of six compound categories as well as $MAE_{365}$ (C).

~~Molecular composition analysis of HULIS identified 264 compounds at the molecular structure level~~Non-targeted analysis of HULIS by UHPLC-HRMS/MS revealed 264 compounds at Schymanski's confidence levels above CL3 (Schymanski et al., 2014). **Table S7** ~~in the supplement~~ listed the details of ~~these~~ detected HULIS compounds and their corresponding CLs~~confidence levels~~. The identified compounds were grouped into six compound categories ~~based on their elemental types~~, including CHO (composed of carbon, hydrogen, and oxygen atoms, hereinafter), CHN, CHON, CHOS, CHONS, and other species. CHONS category refers to compounds that contain carbon, hydrogen, oxygen, nitrogen, and sulfur elements. **Figure 1A and 1C** showed temporal variations of the mass concentrations and fractions ~~six~~of different compound categories. The total mass concentration of these compounds ranged from 1.05 to 7.39 $\mu$g m$^{-3}$ (**Figure 1A**), explaining 38.2% - 78.1% of the total HULIS mass (converted by multiplying [HULIS-C] by 1.6, (Friman et al., 2023)). The remaining unidentified compounds in HULIS mainly include low-polarity phenols, ketones, and aldehydes, which cannot be detected by~~ose polarity is too low to be ionized in~~ the ESI mode (Huang et al., 2025; Huo et al., 2021; Song et al., 2022, 2024).

**Figure 1C** also displayed that MAE at 365 nm ($MAE_{365}$) of HULIS samples. The observed $MAE_{365}$ ranged from 1.28 to 2.12 m$^2$ gC$^{-1}$ (1.81 ± 0.24 m$^2$ gC$^{-1}$ in average), which was higher than those in Beijing (1.79 ± 0.24 m$^2$ gC$^{-1}$) (Cheng et al., 2011), Xi'an (1.65 ± 0.36 m$^2$ gC$^{-1}$) (Huang et al., 2018), Guangzhou (1.1 ± 0.27 m$^2$ gC$^{-1}$) (Zou et al., 2023), and Hong Kong (0.97 ± 0.40 m$^2$ gC$^{-1}$) (Ma et al., 2019) during wintertime~~. This indicated~~, demonstrating that the light absorption efficiency of HULIS in Changchun was~~have~~ higher ~~light absorption efficiency compared to~~than other regions in China. Moreover, the strongly positive correlation (**Figure S7**) between $MAE_{365}$ with CHON category (Pearson's R = 0.75, $p$-value < 0.01) and aromatic fraction (Pearson's R = 0.86, $p$-value < 0.01) suggested that the high light absorption efficiency of HULIS may be related to aromatic CHON compounds.

**3.2 Potential sources of HULIS based on molecular analysis.** To ~~analyze~~ investigate drivers~~the cause~~ of the high concentrations and variable light absorption efficiency of HULIS in this study, we selected two ~~typical haze events~~ samples (Event I and II) among all haze events ($PM_{2.5}$ concentration > 75 $\mu$g m$^{-3}$) that exhibited the maximal divergence~~with significant differences~~ in $MAE_{365}$ values. Event I had higher $PM_{2.5}$ (159.6 ± 53.8 $\mu$g m$^{-3}$) and HULIS-C (6.68 $\mu$gC m$^{-3}$) but lower $MAE_{365,HULIS}$ (~~Event I: $PM_{2.5}$ = 159.6 ± 53.8 $\mu$g m$^{-3}$, $MAE_{365,HULIS}$ =~~ 1.56 m$^2$ gC$^{-1}$~~;~~), while Even II~~:~~ had lower $PM_{2.5}$ (83.7 ± 36.4 $\mu$g m$^{-3}$) and HULIS-C (4.65 $\mu$gC m$^{-3}$) but higher ~~= 83.7 ± 36.4 $\mu$g m$^{-3}$,~~ $MAE_{365,HULIS}$ ~~=~~ (2.06 m$^2$ gC$^{-1}$). These contrasting events were chosen for potential sources comparison from the perspective of molecular composition. Considering the lowest $PM_{2.5}$ and HULIS-C concentration, the sample on January 13 ($PM_{2.5}$ = 14.1 ± 11.9 $\mu$g m$^{-3}$, HULIS-C = 0.97 $\mu$gC m$^{-3}$, $MAE_{365,HULIS}$ = 1.28 m$^2$ gC$^{-1}$) was selected to represent clean days. **Figure 2** exhibited the reconstructed MS spectra, the number, and concentration fraction of HULIS in both positive and negative modes.

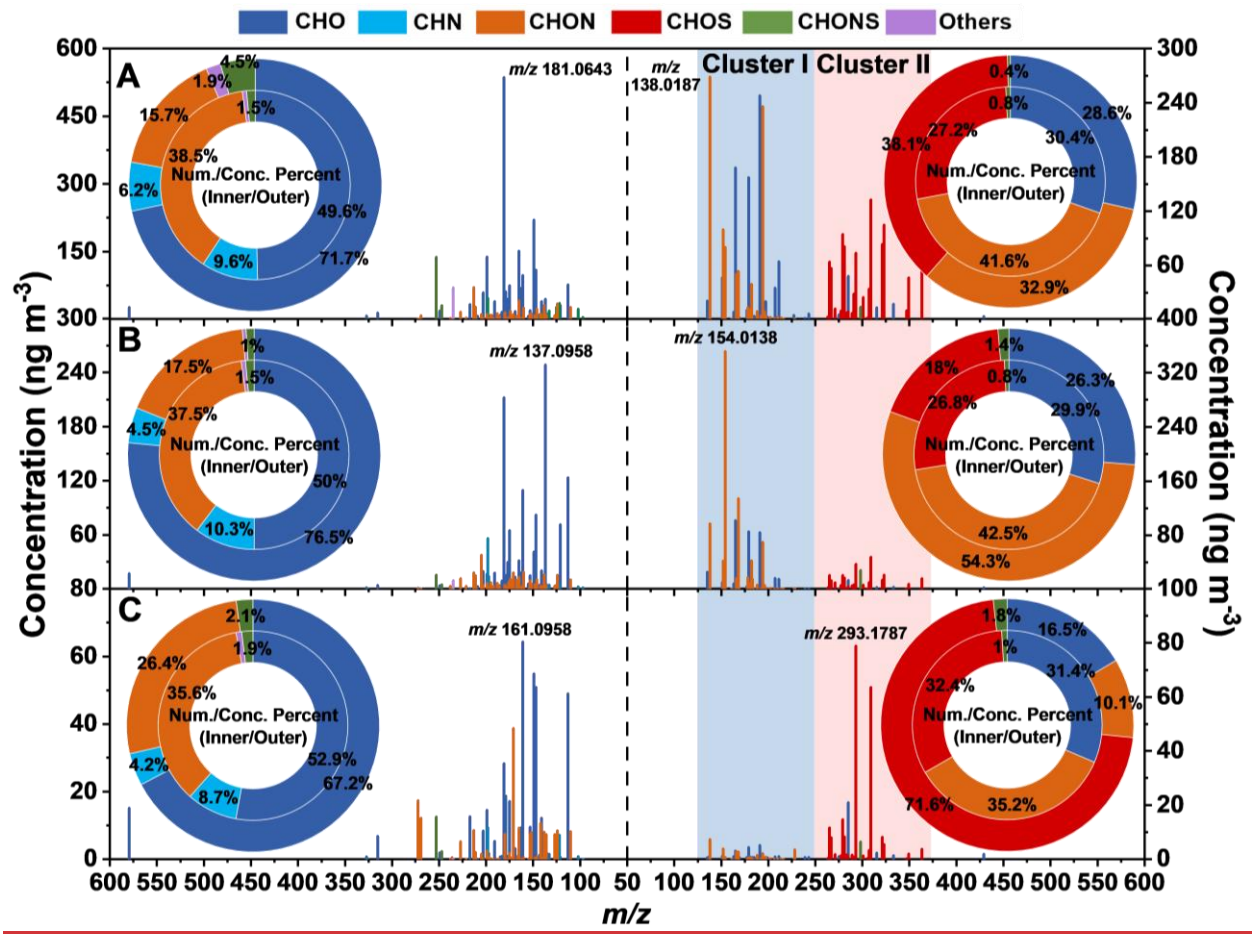


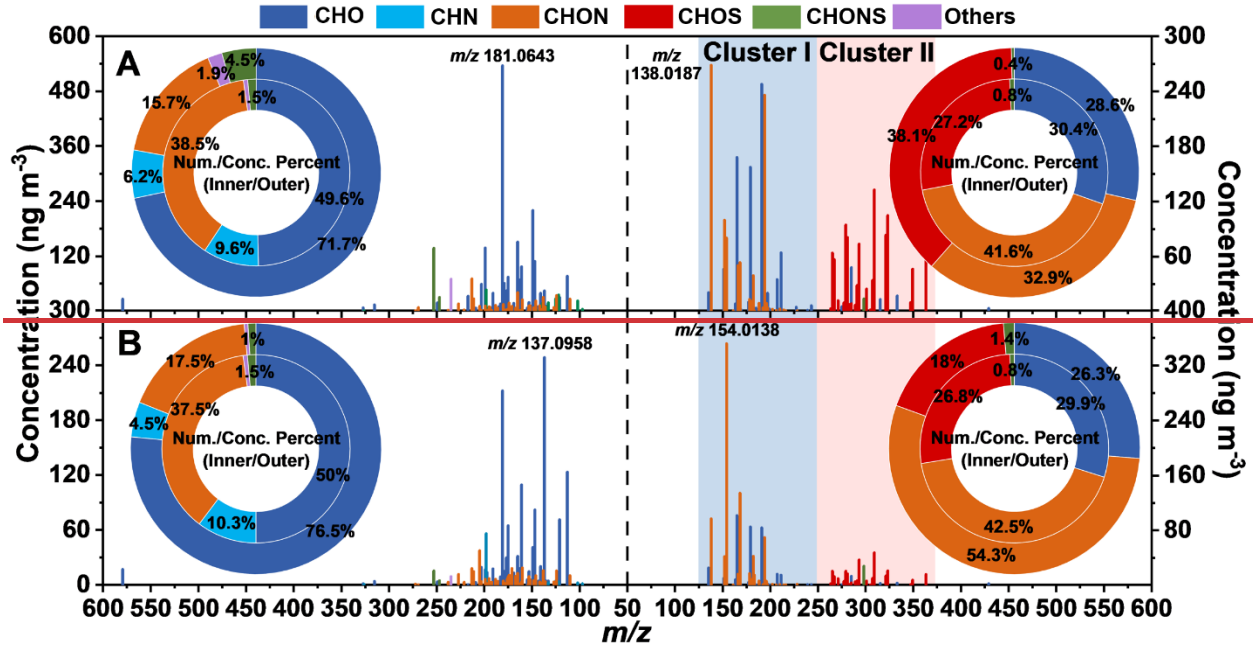


**Figure 2.** Reconstructed mass spectra ~~(positive ions on the left, while negative ions on the right) for the~~ of identified HULIS ~~samples~~ compounds during Event I (A) ~~and~~, Event II (B), and Clean day (C). Spectra are shown for positive ionization mode (left

panels) and negative ionization mode (right panels). *m/z* values increase from middle to both sides in all spectra. The ~~highest peaks~~ most abundant ions are labeled with ~~were marked by~~ their *m/z* values. The accompanying pie charts represent ~~inner and outer ring pie charts were the fraction of mass concentration and numbers in the different categories~~the molecular class distribution of the identified compounds: the inner/outer ring shows the relative abundance based on number/concentration of compounds~~, respectively~~.

In the positive mode, Event I and II had similar ~~elemental~~molecular composition, both dominated by CHO compounds, followed by CHON, CHN, and others. The most abundant species in Event I and II were 9-fluorenone (*m/z* 181.0643) and 2-[(1E)-1-Buten-1-yl]-5-methylfuran (*m/z* 137.0958), respectively. The former originates from diverse combustion sources such as biomass burning, coal combustion, and vehicle emission (Alves et al., 2016; Huo et al., 2021; Ma et al., 2023; Souza et al., 2014; Xu et al., 2024; Zhao et al., 2020), whereas the latter is believed to stem specifically from biomass burning (Bhattu et al., 2019; Hatch et al., 2015). ~~Further evidence for the significant role of biomass burning and coal combustion in both events was provided by the h~~High concentrations of biomass burning ($K^+$) and coal combustion ($SO_2$, **Table S6**) tracers ~~(i.e. vanillin, syringaldehyde, acetosyringone in **Table S6**, and $K^+$ in **Table S5**) and $SO_2$ (**Table S5**)~~ proved the key contribution of biomass burning and coal combustion (Chen et al., 2017; Dutton et al., 2009; He et al., 2010; Liang et al., 2021)~~,~~ ~~Biomass burning and coal combustion~~which have been confirmed in our previous study to be the main sources of air pollution in Changchun winter (Dong et al., 2023).

In the negative mode, two distinct compound clusters were observed within the *m/z* range of 125 – 250 (refer to Cluster I) and 250 – 375 (refer to Cluster II), as marked in the right part of **Figure 2**. Cluster I comprised a significant proportion of strong BrC species, such as nitrophenols (including 4-nitrophenol, 3-nitrocatechol, 4-nitro-1-naphthol, and etc., **Table S7**), mainly originating from primary emissions like biomass burning and coal combustion (Huang et al., 2023; Jiang et al., 2023; Lin et al., 2017; Wang et al., 2020) and secondary formation (Bolzacchini et al., 2001; Mayorga et al., 2021). Notably, the higher abundance of Cluster I in Event II compared to Event I likely contributed to ~~fraction was more prominent in Event II than Event I, explaining~~ the higher $MAE_{365}$ observed during Event II~~in the former~~.

All of CHOS compounds were characterized by ion fragment *m/z* 96.9595 in the MS/MS spectra and were therefore identified as organosulfates (OSs). Cluster II was predominantly composed of OSs, accounting for 84.7 ± 6.5 % of compounds within this cluster during the whole sampling period. Considering the OSs are typically formed by atmospheric aqueous reaction (Brüggemann et al., 2017; Pratt et al., 2013; Wach et al., 2020), ~~we therefore proposed that~~ the dominance of OSs in Cluster II ~~which was mainly composed of OSs originated~~ strongly supports its ~~from~~ secondary formation origin. The higher abundance of Cluster II in Event I ~~suggested that~~ indicated ~~the~~ more intense secondary formation of HULIS ~~was more intense~~ during this event compared to Event II. ~~The~~ This interpretation is corroborated by elevated concentrations of secondary inorganic ions (including $NH_4^+$, $NO_3^-$, and $SO_4^{2-}$, ~~11.35~~16.66 – ~~41.56~~27.66 vs 4.~~30~~49 – 7.~~30~~61 $\mu g\ m^{-3}$) and relative humidity (83.1 ± 4.6% vs 61.9 ± 14.0%) in Event I ~~than those in Event~~vs. II ~~were observed~~, as detailed in **Table S6**. As a result, the higher ALWC (95.9 vs 23.9 $\mu g\ m^{-3}$) and lower pH value (~~4.20~~5.29 vs ~~4.82~~7.31) in Event I in contrast to Event II facilitated the formation of OSs. Since the OSs studied here were primarily aliphatic sulfates (summarized as the molecular formulas of $C_nH_{2n+2}O_{4\text{-}6}S$ and $C_nH_{2n}O_{4\text{-}6}S$, where $10 \leq n \leq 18$), which belong to non-light-absorbing organic matter, this may cause the lower $MAE_{365}$ value in Event I.

**3.3 Effect of ambient temperature on the BrC chromophores of HULIS.** As above-mentioned, the temperature was down to -25℃. This extreme cold temperature critically alters the reactivity, phase partitioning, and

aging kinetics of HULIS(He et al., 2006; Huang et al., 2006; Li and Shiraiwa, 2019; Shiraiwa et al., 2011)~~Such low temperature may affect the evolution of HULIS in the atmosphere~~. In total, 39 compounds were screened as strong BrC chromophores to ~~analyze~~ investigate the effect of temperature on the BrC chromophores according to a partial least squares regression (PLS) model (detailed in **Text S3**). These compounds belong to nitrophenols or nitrophenol derivatives, which are marked in **Table S7**. The mass concentration of these 39 strong BrC chromophores was 0.41 ± 0.27 $\mu$g $m^{-3}$ in average, accounting for ~~accounted for~~ 8.67 ± 3.68% of the total HULIS mass (converted from [HULIS-C] using a factor of 1.6, (Friman et al., 2023)). This mass fraction exceeds values reported for 12 specific nitro-aromatic compounds in previous studies (about 7.5% of HULIS mass, (Frka et al., 2022)). Despite this modest mass contribution, these strong BrC chromophores~~and~~ contributed 28.9 ± 10.4% of the light absorbance (detailed in **Text S4**), with an average $MAE_{365}$ of 7.40 ± 1.80 $m^2$ $gC^{-1}$ (**Figure S7**), ~~indicating their importance in the light absorption of HULIS~~higher than 10% and 14% light absorbance contribution of 18 chromophores in Xi'an and Beijing (Huang et al., 2020).

**Figure 3** ~~presented~~shows that the mass fraction of screened 39 strong BrC chromophores under different temperature ranges, as well as the negative variation patterns between~~, along with~~ the $MAE_{365}$ and ambient temperature~~value of HULIS~~. In contrast, the $OC_{com}/OC_{total}$ ratio shows no consistent temperature dependence~~, across different temperature ranges. Both mass fraction and $MAE_{365}$ increased with decreasing ambient temperature, indicating that~~ suggesting low temperature rather than combustion emission ~~may facilitate~~promote the accumulation of strong BrC species in the particle~~s phase~~. We proposed two possible explanations: firstly, the low temperature may lead to a non-liquid ~~phase~~ state of ambient particles, potentially introducing kinetic limitation on the diffusion of reactive species from gas phase into particle bulk (Li and Shiraiwa, 2019). We utilized an established parameterization scheme (**Text S5**) to calculate the glass transition temperature (Tg) of HULIS based on their molecular composition (Li et al., 2020). The results showed that the decrease in ambient temperature (T) enhanced the Tg/T ratio, driving the phase transition of particles from liquid state (Tg/T = 0.76) to semi-solid state (Tg/T > 0.79). This may lead to the diffusion coefficients reduction of reactive species (Arangio et al., 2015; Gatzsche et al., 2017; Mikhailov et al., 2009; Shiraiwa et al., 2011; Virtanen et al., 2010), thereby slowing the degradation rate of BrC via hydroxyl radical oxidation or triplet excitation pathways in the atmosphere (Schnitzler et al., 2022; Schnitzler and Abbatt, 2018). These findings suggest that the non-liquid particle phase state, ~~in conjunction~~accompanied with the weak solar radiation during Changchun's winter (refer to **Figure 1B**), results in a less pronounced photochemical aging of BrC, thereby diminishing its photobleaching.

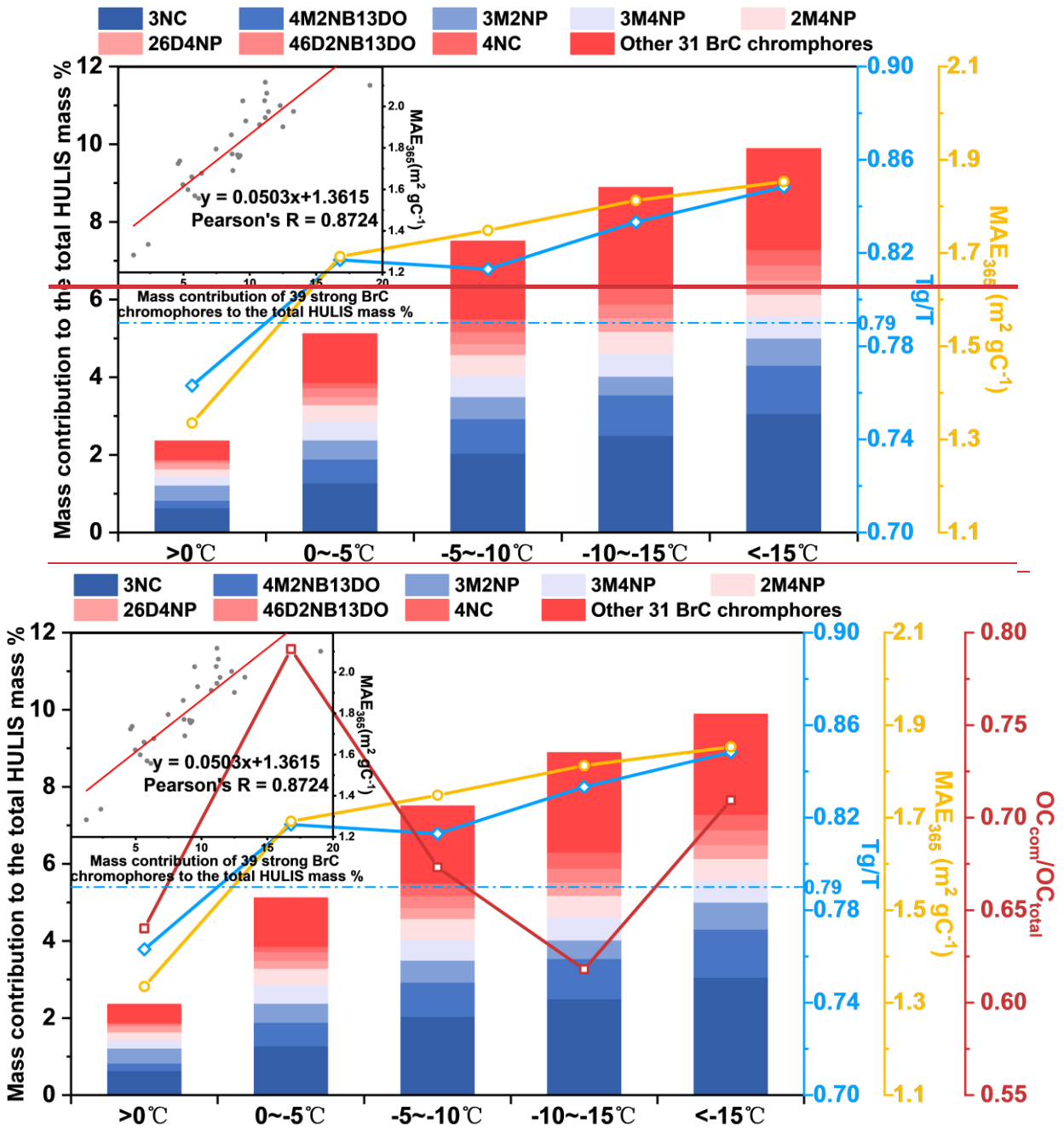


**Figure 3.** Temperature-dependent variations in mass fraction of 39 strong BrC chromophores, $MAE_{365}$ value of HULIS, Tg/T ratio, and $OC_{com}/OC_{total}$ ratio, with correlation between chromophore mass fraction and HULIS $MAE_{365}$. ~~The mass contribution of 39 strong BrC chromophores, $MAE_{365}$ values, ratios of glass transition temperature (Tg) to temperature (T) at different temperatures, and linear relationships between mass contribution of strong BrC and $MAE_{365}$ of HULIS.~~ The blue dotted line represented the threshold of Tg/T between liquid and semi-solid state (Shiraiwa et al., 2017), and the abbreviations of 3NC, 4M2NB13DO, 3M2NP, 3M4NP, 2M4NP, 26D4NP, 46D2NB13DO, and 4NC represents 3-nitrocatechol, 4-methyl-2-nitrobenzene-1,3-diol, 3-methyl-2-nitrophenol, 3-methyl-4-nitrophenol, 2-methyl-4-nitrophenol, 2,6-dimethyl-4-nitrophenol, 4,6-dimethyl-2-nitrobenzene-1,3-diol, and 4-nitrocatechol, respectively.

Secondly, the formation of BrC chromophores was also important for the $MAE_{365}$ enhancement of HULIS. On

the one hand, the secondary formation of nitrophenols has been conclusively attributed to reaction of phenols with $NO_x$ radicals (Bolzacchini et al., 2001; Finewax et al., 2018; Kroflič et al., 2021; Mayorga et al., 2021), a process that has been characterized as exothermic (Bolzacchini et al., 2001; Domingo et al., 2021). On the other hand, we have demonstrated that further atmospheric oxidation of nitrophenols proceeds via a ring-opening mechanism of benzene moiety (Qiu et al., 2024), which constitutes an endothermic reaction (Cao et al., 2021; Hems and Abbatt, 2018; Wang et al., 2017). From a thermodynamic perspective, low temperature not only promotes exothermic ~~chemical reactions~~formation of nitrophenols while~~but also~~ simultaneously suppressing~~hinders~~ their endothermic degradation via ring-opening~~processes, thereby accumulating the strong BrC chromophores such as nitrophenols in HULIS~~. Furthermore, low temperature inhibits the volatilization and enhances the particle-phase retention of these volatile chromophores (He et al., 2006; Huang et al., 2006). This combined effect of low temperature led to the accumulation of strong BrC chromophores like nitrophenols within HULIS. This mechanism is consistent with field observations of enhanced nitroaromatic abundance in winter aerosols (Cai et al., 2022; Teich et al., 2017; Zhang et al., 2024). As such, we infer that ambient temperature plays a critical role in promoting the transformation and light absorption of BrC chromophores, particularly in cold or/and high-altitude regions.

**3.4 Conclusions.** In this work, we explored the linkage between the light absorption and molecular structure of atmospheric HULIS in Changchun winter based on UHPLC-HRMS/MS. In different haze events, the molecular structure of HULIS varied due to different sources, which lead to differences in their light absorption efficiency. Biomass burning and coal combustion were important inducers of the high $MAE_{365}$ value of HULIS. It was the fact that biomass burning and coal combustion emitted a large fraction of BrC chromophores such as nitrophenols, while aliphatic organosulfates produced by secondary formation lead to the reduction in the light absorption efficiency of HULIS.

In addition, our study screened out 39 strong BrC chromophores belonging to nitrophenols by PLS model. These species accounted for 8.67 ± 3.68% of the total HULIS mass while contributed nearly 30% of the light absorbance at 365 nm. We found that low temperature can promote the accumulation of strong BrC chromophores through slowing down the photobleaching reaction and changing the thermodynamic reaction equilibrium, thereby improving the light absorption capability of HULIS. This phenomenon has not been studied before, and further laboratory and field studies are urgently needed to verify the effect of temperature on the light absorption properties of BrC.

Our research has found that in the cold regions of northern China, on one hand, primary emissions from biomass burning and coal combustion are relatively strong, and on the other hand, low temperatures reduce the photobleaching of brown carbon (BrC). This implies that BrC in cold regions may have a longer lifetime and stronger light-absorbing properties in the atmosphere, thus playing a more significant role in the direct radiative forcing of carbonaceous aerosols.

**Supplementary Information.** Optimization details of LC-MS method, calculation procedure of relevant index, screening details of PLS model, and analysis results of pollutant data and meteorological data (PDF).

The information about atmospheric mass concentration, molecular information, and strong brown carbon chromophores of identified compounds in HULIS samples of Changchun during wintertime (Table S7).

**Author Contributions.** T. Q. and Y. Q. designed this work. T. Q., X. W., and Y. G., collected the experimental samples. T. Q., Y. Q., Y. Y., R. S., Y. N., X. H., and X. M. collected and analyzed the experimental data. Z. W., D. L., D. D., and

J. M. edited the manuscript. All authors have read and agreed to the published version of the manuscript.

**Funding.** This work was supported by the National Natural Science Foundation of China (No. 22376084) and Environmental Protection Research Program from Jilin Department of Ecology and Environment (No. 2023-09).

**Notes.** The authors declare no competing financial interest.

**Acknowledgments.** Authors of this article wish to thank the financial support from the National Natural Science Foundation of China (No. 22376084) and Environmental Protection Research Program from Jilin Department of Ecology and Environment (No. 2023-09), the technical support from Ms. Huimin Qian and the work support from Mr. Shengao Yang. This work was also supported by State key Laboratory of Inorganic Synthesis and Preparation Chemistry, Jilin University.

## Reference


Allen, F., Greiner, R., and Wishart, D.: Competitive fragmentation modeling of ESI-MS/MS spectra for putative metabolite identification, Metabolomics, 11, 98–110, https://doi.org/10.1007/S11306-014-0676-4, 2015.

Alves, C. A., Vicente, A. M. P., Gomes, J., Nunes, T., Duarte, M., and Bandowe, B. A. M.: Polycyclic aromatic hydrocarbons (PAHs) and their derivatives (oxygenated-PAHs, nitrated-PAHs and azaarenes) in size-fractionated particles emitted in an urban road tunnel, Atmos Res, 180, 128–137, https://doi.org/10.1016/J.ATMOSRES.2016.05.013, 2016.

Arangio, A. M., Slade, J. H., Berkemeier, T., Pöschl, U., Knopf, D. A., and Shiraiwa, M.: Multiphase chemical kinetics of oh radical uptake by molecular organic markers of biomass burning aerosols: Humidity and temperature dependence, surface reaction, and bulk diffusion, Journal of Physical Chemistry A, 119, 4533–4544, https://doi.org/10.1021/JP510489Z, 2015.

Arp, H. P. H., Schwarzenbach, R. P., and Goss, K. U.: Ambient gas/particle partitioning. 2: The influence of particle source and temperature on sorption to dry terrestrial aerosols, Environ Sci Technol, 42, 5951–5957, https://doi.org/10.1021/ES703096P, 2008.

Baduel, C., Voisin, D., and Jaffrezo, J. L.: Comparison of analytical methods for humic Like Substances (HULIS) measurements in atmospheric particles, Atmos Chem Phys, 9, 5949–5962, https://doi.org/10.5194/ACP-9-5949-2009, 2009.

Bao, M., Zhang, Y. L., Cao, F., Hong, Y., Lin, Y. C., Yu, M., Jiang, H., Cheng, Z., Xu, R., and Yang, X.: Impact of fossil and non-fossil fuel sources on the molecular compositions of water-soluble humic-like substances in PM2.5 at a suburban site of Yangtze River Delta, China, Atmos Chem Phys, 23, 8305–8324, https://doi.org/10.5194/ACP-23-8305-2023, 2023.

Bhattu, D., Zotter, P., Zhou, J., Stefenelli, G., Klein, F., Bertrand, A., Temime-Roussel, B., Marchand, N., Slowik, J. G., Baltensperger, U., Prevot, A. S. H., Nussbaumer, T., Haddad, I. El, and Dommen, J.: Effect of Stove Technology and Combustion Conditions on Gas and Particulate Emissions from Residential Biomass Combustion, Environ Sci Technol, 53, 2209–2219, https://doi.org/10.1021/ACS.EST.8B05020, 2019.

Bolzacchini, E., Bruschi, M., Hjorth, J., Meinardi, S., Orlandi, M., Rindone, B., and Rosenbohm, E.: Gas-phase reaction of phenol with NO3, Environ Sci Technol, 35, 1791–1797, https://doi.org/10.1021/ES001290M, 2001.

Brüggemann, M., Poulain, L., Held, A., Stelzer, T., Zuth, C., Richters, S., Mutzel, A., Van Pinxteren, D., Iinuma, Y., Katkevica, S., Rabe, R., Herrmann, H., and Hoffmann, T.: Real-time detection of highly oxidized organosulfates and BSOA marker compounds during the F-BEACh 2014 field study, Atmos Chem Phys, 17, 1453–1469, https://doi.org/10.5194/ACP-17-1453-2017, 2017.

Cabada, J. C., Pandis, S. N., Subramanian, R., Robinson, A. L., Polidori, A., and Turpin, B.: Estimating the Secondary Organic Aerosol Contribution to PM2.5 Using the EC Tracer Method Special Issue of Aerosol Science and Technology on Findings from the Fine Particulate Matter Supersites Program, Aerosol Science and Technology, 38, 140–155, https://doi.org/10.1080/02786820390229084, 2004.

Cai, D., Wang, X., George, C., Cheng, T., Herrmann, H., Li, X., and Chen, J.: Formation of Secondary Nitroaromatic Compounds in Polluted Urban Environments, Journal of Geophysical Research: Atmospheres, 127, e2021JD036167, https://doi.org/10.1029/2021JD036167, 2022.

Cao, L. M., Huang, X. F., Li, Y. Y., Hu, M., and He, L. Y.: Volatility measurement of atmospheric submicron aerosols in an urban atmosphere in southern China, Atmos Chem Phys, 18, 1729–1743, https://doi.org/10.5194/ACP-18-1729-2018, 2018.

Cao, T. ting, Xu, T. fu, Deng, F. xia, Qiao, W. wei, and Cui, C. wei: Reactivity and mechanism between OH and phenolic pollutants: Efficiency and DFT calculation, J Photochem Photobiol A Chem, 407, 113025, https://doi.org/10.1016/J.JPHOTOCHEM.2020.113025, 2021.

Cappiello, A., De Simoni, E., Fiorucci, C., Mangani, F., Palma, P., Trufelli, H., Decesari, S., Facchini, M. C., and Fuzzi, S.: Molecular characterization of the water-soluble organic compounds in fogwater by ESIMS/MS, Environ Sci Technol, 37, 1229–1240, https://doi.org/10.1021/ES0259990, 2003.s

Chen, J., Wu, Z. J., Zhao, X., Wang, Y. J., Chen, J. C., Qiu, Y. T., Zong, T. M., Chen, H. X., Wang, B. B., Lin, P., Liu, W., Guo, S., Yao, M. S., Zeng, L. M., Wex, H., Liu, X., Hu, M., and Li, S. M.: Atmospheric Humic-Like Substances (HULIS) Act as Ice Active Entities, Geophys Res Lett, 48, e2021GL092443, https://doi.org/10.1029/2021GL092443, 2021.

Chen, S., Guo, Z., Guo, Z., Guo, Q., Zhang, Y., Zhu, B., and Zhang, H.: Sulfur isotopic fractionation and its implication: Sulfate formation in PM2.5 and coal combustion under different conditions, Atmos Res, 194, 142–149, https://doi.org/10.1016/J.ATMOSRES.2017.04.034, 2017.

Cheng, Y., He, K. B., Zheng, M., Duan, F. K., Du, Z. Y., Ma, Y. L., Tan, J. H., Yang, F. M., Liu, J. M., Zhang, X. L., Weber, R. J., Bergin, M. H., and Russell, A. G.: Mass absorption efficiency of elemental carbon and water-soluble organic carbon in Beijing, China, Atmos Chem Phys, 11, 11497–11510, https://doi.org/10.5194/ACP-11-11497-2011, 2011.

Chung, C. E., Ramanathan, V., and Decremer, D.: Observationally constrained estimates of carbonaceous aerosol radiative forcing, Proc Natl Acad Sci U S A, 109, 11624–11629, https://doi.org/10.1073/PNAS.1203707109, 2012.

Domingo, L. R., Seif, A., Mazarei, E., Zahedi, E., and Ahmadi, T. S.: Quasi-RRHO approximation and DFT study for understanding the mechanism and kinetics of nitration reaction of benzonitrile with nitronium ion, Comput Theor Chem, 1199, 113209, https://doi.org/10.1016/J.COMPTC.2021.113209, 2021.

Dong, D., Qiu, T., Du, S., Gu, Y., Li, A., Hua, X., Ning, Y., and Liang, D.: The chemical characterization and source apportionment of PM2.5 and PM10 in a typical city of Northeast China, Urban Clim, 47, 101373, https://doi.org/10.1016/J.UCLIM.2022.101373, 2023.

Dou, J., Lin, P., Kuang, B. Y., and Yu, J. Z.: Reactive oxygen species production mediated by humic-like substances in atmospheric aerosols: Enhancement effects by pyridine, imidazole, and their derivatives, Environ Sci Technol, 49, 6457–6465, https://doi.org/10.1021/ES5059378, 2015.

Dutton, S. J., Williams, D. E., Garcia, J. K., Vedal, S., and Hannigan, M. P.: PM2.5 characterization for time series studies: Organic molecular marker speciation methods and observations from daily measurements in Denver, Atmos Environ, 43, 2018–2030, https://doi.org/10.1016/J.ATMOSENV.2009.01.003, 2009.

Emmenegger, C., Reinhardt, A., Hueglin, C., Zenobi, R., and Kalberer, M.: Evaporative light scattering: A novel detection method for the quantitative analysis of humic-like substances in aerosols, Environ Sci Technol, 41, 2473–2478, https://doi.org/10.1021/ES061095T, 2007.

Finewax, Z., De Gouw, J. A., and Ziemann, P. J.: Identification and Quantification of 4-Nitrocatechol Formed from OH and NO3 Radical-Initiated Reactions of Catechol in Air in the Presence of NOx: Implications for Secondary Organic Aerosol Formation from Biomass Burning, Environ Sci Technol, 52, 1981–1989, https://doi.org/10.1021/ACS.EST.7B05864, 2018.

Fountoukis, C. and Nenes, A.: ISORROPIAII: A computationally efficient thermodynamic equilibrium model for K+-Ca2+-Mg2+-NH4+-Na+-SO42--NO3--Cl--H2O aerosols, Atmos Chem Phys, 7, 4639–4659,

https://doi.org/10.5194/ACP-7-4639-2007, 2007.
Friman, M., Aurela, M., Saarnio, K., Teinilä, K., Kesti, J., Harni, S. D., Saarikoski, S., Hyvärinen, A., and Timonen, H.: Long-term characterization of organic and elemental carbon at three different background areas in northern Europe, Atmos Environ, 310, 119953, https://doi.org/10.1016/J.ATMOSENV.2023.119953, 2023.
Frka, S., Šala, M., Brodnik, H., Štefane, B., Kroflič, A., and Grgić, I.: Seasonal variability of nitroaromatic compounds in ambient aerosols: Mass size distribution, possible sources and contribution to water-soluble brown carbon light absorption, Chemosphere, 299, 134381, https://doi.org/10.1016/J.CHEMOSPHERE.2022.134381, 2022.
Gatzsche, K., Iinuma, Y., Tilgner, A., Mutzel, A., Berndt, T., and Wolke, R.: Kinetic modeling studies of SOA formation from ?-pinene ozonolysis, Atmos Chem Phys, 17, 13187–13211, https://doi.org/10.5194/ACP-17-13187-2017, 2017.
Gregson, F. K. A., Gerrebos, N. G. A., Schervish, M., Nikkho, S., Schnitzler, E. G., Schwartz, C., Carlsten, C., Abbatt, J. P. D., Kamal, S., Shiraiwa, M., and Bertram, A. K.: Phase Behavior and Viscosity in Biomass Burning Organic Aerosol and Climatic Impacts, Environ Sci Technol, 57, 14548–14557, https://doi.org/10.1021/ACS.EST.3C03231, 2023.
Hatch, L. E., Luo, W., Pankow, J. F., Yokelson, R. J., Stockwell, C. E., and Barsanti, K. C.: Identification and quantification of gaseous organic compounds emitted from biomass burning using two-dimensional gas chromatography-time-of-flight mass spectrometry, Atmos Chem Phys, 15, 1865–1899, https://doi.org/10.5194/ACP-15-1865-2015, 2015.
He, J., Zielinska, B., and Balasubramanian, R.: Composition of semi-volatile organic compounds in the urban atmosphere of Singapore: Influence of biomass burning, Atmos Chem Phys, 10, 11401–11413, https://doi.org/10.5194/ACP-10-11401-2010, 2010.
He, L. Y., Hu, M., Huang, X. F., Zhang, Y. H., and Tang, X. Y.: Seasonal pollution characteristics of organic compounds in atmospheric fine particles in Beijing, Science of The Total Environment, 359, 167–176, https://doi.org/10.1016/J.SCITOTENV.2005.05.044, 2006.
Heald, C. L., Jacob, D. J., Park, R. J., Russell, L. M., Huebert, B. J., Seinfeld, J. H., Liao, H., and Weber, R. J.: A large organic aerosol source in the free troposphere missing from current models, Geophys Res Lett, 32, 1–4, https://doi.org/10.1029/2005GL023831, 2005.
Hems, R. F. and Abbatt, J. P. D.: Aqueous Phase Photo-oxidation of Brown Carbon Nitrophenols: Reaction Kinetics, Mechanism, and Evolution of Light Absorption, ACS Earth Space Chem, 2, 225–234, https://doi.org/10.1021/ACSEARTHSPACECHEM.7B00123, 2018.
Hems, R. F., Schnitzler, E. G., Liu-Kang, C., Cappa, C. D., and Abbatt, J. P. D.: Aging of Atmospheric Brown Carbon Aerosol, ACS Earth Space Chem, 5, 722–748, https://doi.org/10.1021/ACSEARTHSPACECHEM.0C00346, 2021.
Hoffer, A., Gelencsér, A., Guyon, P., Kiss, G., Schmid, O., Frank, G. P., Artaxo, P., and Andreae, M. O.: Optical properties of humic-like substances (HULIS) in biomass-burning aerosols, Atmos Chem Phys, 6, 3563–3570, https://doi.org/10.5194/ACP-6-3563-2006, 2006.
Huang, L., Wang, J., Jiang, H., Chen, L., and Chen, H.: On-line determination of selenium compounds in tea infusion by extractive electrospray ionization mass spectrometry combined with a heating reaction device, Chinese Chemical Letters, 36, 109896, https://doi.org/10.1016/J.CCLET.2024.109896, 2025.
Huang, R. J., Yang, L., Cao, J., Chen, Y., Chen, Q., Li, Y., Duan, J., Zhu, C., Dai, W., Wang, K., Lin, C., Ni, H.,

Corbin, J. C., Wu, Y., Zhang, R., Tie, X., Hoffmann, T., O'Dowd, C., and Dusek, U.: Brown Carbon Aerosol in Urban Xi'an, Northwest China: The Composition and Light Absorption Properties, Environ Sci Technol, 52, 6825–6833, https://doi.org/10.1021/ACS.EST.8B02386, 2018.

Huang, R. J., Yang, L., Shen, J., Yuan, W., Gong, Y., Guo, J., Cao, W., Duan, J., Ni, H., Zhu, C., Dai, W., Li, Y., Chen, Y., Chen, Q., Wu, Y., Zhang, R., Dusek, U., O'Dowd, C., and Hoffmann, T.: Water-Insoluble Organics Dominate Brown Carbon in Wintertime Urban Aerosol of China: Chemical Characteristics and Optical Properties, Environ Sci Technol, 54, 7836–7847, https://doi.org/10.1021/acs.est.0c01149, 2020.

Huang, S., Yang, X., Xu, H., Zeng, Y., Li, D., Sun, J., Ho, S. S. H., Zhang, Y., Cao, J., and Shen, Z.: Insights into the nitroaromatic compounds, formation, and light absorption contributing emissions from various geological maturity coals, Science of The Total Environment, 870, 162033, https://doi.org/10.1016/J.SCITOTENV.2023.162033, 2023.

Huang, X. F., He, L. Y., Hu, M., and Zhang, Y. H.: Annual variation of particulate organic compounds in PM2.5 in the urban atmosphere of Beijing, Atmos Environ, 40, 2449–2458, https://doi.org/10.1016/J.ATMOSENV.2005.12.039, 2006.

Huo, Y., Guo, Z., Li, Q., Wu, D., Ding, X., Liu, A., Huang, D., Qiu, G., Wu, M., Zhao, Z., Sun, H., Song, W., Li, X., Chen, Y., Wu, T., and Chen, J.: Chemical Fingerprinting of HULIS in Particulate Matters Emitted from Residential Coal and Biomass Combustion, Environ Sci Technol, 55, 3593–3603, https://doi.org/10.1021/acs.est.0c08518, 2021.

Jiang, H., Cai, J., Feng, X., Chen, Y., Wang, L., Jiang, B., Liao, Y., Li, J., Zhang, G., Mu, Y., and Chen, J.: Aqueous-Phase Reactions of Anthropogenic Emissions Lead to the High Chemodiversity of Atmospheric Nitrogen-Containing Compounds during the Haze Event, Environ Sci Technol, 57, 16500–16511, https://doi.org/10.1021/ACS.EST.3C06648, 2023.

Kind, T. and Fiehn, O.: Seven Golden Rules for heuristic filtering of molecular formulas obtained by accurate mass spectrometry, BMC Bioinformatics, 8, https://doi.org/10.1186/1471-2105-8-105, 2007.

Krivácsy, Z., Kiss, G., Varga, B., Galambos, I., Sárvári, Z., Gelencsér, A., Molnár, Á., Fuzzi, S., Facchini, M. C., Zappoli, S., Andracchio, A., Alsberg, T., Hansson, H. C., and Persson, L.: Study of humic-like substances in fog and interstitial aerosol by size-exclusion chromatography and capillary electrophoresis, Atmos Environ, 34, 4273–4281, https://doi.org/10.1016/S1352-2310(00)00211-9, 2000.

Kroflič, A., Anders, J., Drventić, I., Mettke, P., Böge, O., Mutzel, A., Kleffmann, J., and Herrmann, H.: Guaiacol Nitration in a Simulated Atmospheric Aerosol with an Emphasis on Atmospheric Nitrophenol Formation Mechanisms, ACS Earth Space Chem, 5, 1083–1093, https://doi.org/10.1021/ACSEARTHSPACECHEM.1C00014, 2021.

Kuang, Y., Shang, J., Sheng, M., Shi, X., Zhu, J., and Qiu, X.: Molecular Composition of Beijing PM2.5 Brown Carbon Revealed by an Untargeted Approach Based on Gas Chromatography and Time-of-Flight Mass Spectrometry, Environ Sci Technol, 57, 909–919, https://doi.org/10.1021/acs.est.2c05918, 2023.

Laskin, A., Laskin, J., and Nizkorodov, S. A.: Chemistry of Atmospheric Brown Carbon, Chem Rev, 115, 4335–4382, https://doi.org/10.1021/CR5006167, 2015.

Li, Y. and Shiraiwa, M.: Timescales of secondary organic aerosols to reach equilibrium at various temperatures and relative humidities, Atmos Chem Phys, 19, 5959–5971, https://doi.org/10.5194/ACP-19-5959-2019, 2019.

Li, Y., A. Day, D., Stark, H., L. Jimenez, J., and Shiraiwa, M.: Predictions of the glass transition temperature and viscosity of organic aerosols from volatility distributions, Atmos Chem Phys, 20, 8103–8122,

https://doi.org/10.5194/ACP-20-8103-2020, 2020.
Liang, L., Engling, G., Liu, C., Xu, W., Liu, X., Cheng, Y., Du, Z., Zhang, G., Sun, J., and Zhang, X.: Measurement report: Chemical characteristics of PM2.5 during typical biomass burning season at an agricultural site of the North China Plain, Atmos Chem Phys, 21, 3181–3192, https://doi.org/10.5194/ACP-21-3181-2021, 2021.
Limbeck, A., Handler, M., Neuberger, B., Klatzer, B., and Puxbaum, H.: Carbon-specific analysis of humic-like substances in atmospheric aerosol and precipitation samples, Anal Chem, 77, 7288–7293, https://doi.org/10.1021/AC050953L, 2005.
Lin, P., Bluvshtein, N., Rudich, Y., Nizkorodov, S. A., Laskin, J., and Laskin, A.: Molecular Chemistry of Atmospheric Brown Carbon Inferred from a Nationwide Biomass Burning Event, Environ Sci Technol, 51, 11561–11570, https://doi.org/10.1021/ACS.EST.7B02276, 2017.
Liu, J., Scheuer, E., Dibb, J., Ziemba, L. D., Thornhill, K. L., Anderson, B. E., Wisthaler, A., Mikoviny, T., Devi, J. J., Bergin, M., and Weber, R. J.: Brown carbon in the continental troposphere, Geophys Res Lett, 41, 2191–2195, https://doi.org/10.1002/2013GL058976, 2014.
Liu, W., Liao, K., Chen, Q., He, L., Liu, Y., and Kuwata, M.: Existence of Crystalline Ammonium Sulfate Nuclei Affects Chemical Reactivity of Oleic Acid Particles Through Heterogeneous Nucleation, Journal of Geophysical Research: Atmospheres, 128, e2023JD038675, https://doi.org/10.1029/2023JD038675, 2023.
Lu, S., Win, M. S., Zeng, J., Yao, C., Zhao, M., Xiu, G., Lin, Y., Xie, T., Dai, Y., Rao, L., Zhang, L., Yonemochi, S., and Wang, Q.: A characterization of HULIS-C and the oxidative potential of HULIS and HULIS-Fe(II) mixture in PM2.5 during hazy and non-hazy days in Shanghai, Atmos Environ, 219, 117058, https://doi.org/10.1016/J.ATMOSENV.2019.117058, 2019.
Ma, G., Liu, X., Wang, J., Li, M., Dong, Z., Li, X., Wang, L., Han, Y., and Cao, J.: Characteristics and health risk assessment of indoor and outdoor PM2.5 in a rural village, in Northeast of China: impact of coal and biomass burning, Environ Geochem Health, 45, 9639–9652, https://doi.org/10.1007/S10653-023-01755-W, 2023.
Ma, Y., Cheng, Y., Qiu, X., Cao, G., Kuang, B., Yu, J. Z., and Hu, D.: Optical properties, source apportionment and redox activity of humic-like substances (HULIS) in airborne fine particulates in Hong Kong, Environmental Pollution, 255, 113087, https://doi.org/10.1016/J.ENVPOL.2019.113087, 2019.
Mayorga, R. J., Zhao, Z., and Zhang, H.: Formation of secondary organic aerosol from nitrate radical oxidation of phenolic VOCs: Implications for nitration mechanisms and brown carbon formation, Atmos Environ, 244, 117910, https://doi.org/10.1016/J.ATMOSENV.2020.117910, 2021.
Mikhailov, E., Vlasenko, S., Martin, S. T., Koop, T., and Pöschl, U.: Amorphous and crystalline aerosol particles interacting with water vapor: Conceptual framework and experimental evidence for restructuring, phase transitions and kinetic limitations, Atmos Chem Phys, 9, 9491–9522, https://doi.org/10.5194/ACP-9-9491-2009, 2009.
Nenes, A., Pandis, S. N., and Pilinis, C.: ISORROPIA: A new thermodynamic equilibrium model for multiphase multicomponent inorganic aerosols, Aquat Geochem, 4, 123–152, https://doi.org/10.1023/A:1009604003981, 1998.
Nguyen, Q. T., Christensen, M. K., Cozzi, F., Zare, A., Hansen, A. M. K., Kristensen, K., Tulinius, T. E., Madsen, H. H., Christensen, J. H., Brandt, J., Massling, A., Nøjgaard, J. K., and Glasius, M.: Understanding the anthropogenic influence on formation of biogenic secondary organic aerosols in Denmark via analysis of organosulfates and related oxidation products, Atmos Chem Phys, 14, 8961–8981, https://doi.org/10.5194/ACP-

14-8961-2014, 2014.
Nozière, B., Kalberer, M., Claeys, M., Allan, J., D'Anna, B., Decesari, S., Finessi, E., Glasius, M., Grgić, I., Hamilton, J. F., Hoffmann, T., Iinuma, Y., Jaoui, M., Kahnt, A., Kampf, C. J., Kourtchev, I., Maenhaut, W., Marsden, N., Saarikoski, S., Schnelle-Kreis, J., Surratt, J. D., Szidat, S., Szmigielski, R., and Wisthaler, A.: The Molecular Identification of Organic Compounds in the Atmosphere: State of the Art and Challenges, Chem Rev, 115, 3919–3983, https://doi.org/10.1021/CR5003485, 2015.
Pani, S. K., Lee, C. Te, Griffith, S. M., and Lin, N. H.: Humic-like substances (HULIS) in springtime aerosols at a high-altitude background station in the western North Pacific: Source attribution, abundance, and light-absorption, Science of The Total Environment, 809, 151180, https://doi.org/10.1016/J.SCITOTENV.2021.151180, 2022.
Pratt, K. A., Fiddler, M. N., Shepson, P. B., Carlton, A. G., and Surratt, J. D.: Organosulfates in cloud water above the Ozarks' isoprene source region, Atmos Environ, 77, 231–238, https://doi.org/10.1016/J.ATMOSENV.2013.05.011, 2013.
Qin, J., Zhang, L., Qin, Y., Shi, S., Li, J., Gao, Y., Tan, J., and Wang, X.: PH-Dependent Chemical Transformations of Humic-Like Substances and Further Cognitions Revealed by Optical Methods, Environ Sci Technol, 56, 7578–7587, https://doi.org/10.1021/ACS.EST.1C07729, 2022.
Qiu, Y., Qiu, T., Wu, Z., Liu, Y., Fang, W., Man, R., Liu, Y., Wang, J., Meng, X., Chen, J., Liang, D., Guo, S., and Hu, M.: Observational Evidence of Brown Carbon Photobleaching in Urban Atmosphere at Molecular Level, Environ Sci Technol Lett, https://doi.org/10.1021/ACS.ESTLETT.4C00647, 2024.
Roelofs, G. J.: A steady-state analysis of the temperature responses of water vapor and aerosol lifetimes, Atmos Chem Phys, 13, 8245–8254, https://doi.org/10.5194/ACP-13-8245-2013, 2013.
Schervish, M. and Donahue, N. M.: Peroxy radical chemistry and the volatility basis set, Atmos Chem Phys, 20, 1183–1199, https://doi.org/10.5194/ACP-20-1183-2020, 2020.
Schnitzler, E. G. and Abbatt, J. P. D.: Heterogeneous OH oxidation of secondary brown carbon aerosol, Atmos Chem Phys, 18, 14539–14553, https://doi.org/10.5194/ACP-18-14539-2018, 2018.
Schnitzler, E. G., Gerrebos, N. G. A., Carter, T. S., Huang, Y., Heald, C. L., Bertram, A. K., and Abbatt, J. P. D.: Rate of atmospheric brown carbon whitening governed by environmental conditions, Proc Natl Acad Sci U S A, 119, e2205610119, https://doi.org/10.1073/PNAS.2205610119, 2022.
Schymanski, E. L., Jeon, J., Gulde, R., Fenner, K., Ruff, M., Singer, H. P., and Hollender, J.: Identifying small molecules via high resolution mass spectrometry: Communicating confidence, https://doi.org/10.1021/es5002105, 2014.
Serafeim, E., Besis, A., Kouras, A., Farias, C. N., Yera, A. B., Pereira, G. M., Samara, C., and de Castro Vasconcellos, P.: Oxidative potential of ambient PM2.5 from São Paulo, Brazil: Variations, associations with chemical components and source apportionment, Atmos Environ, 298, 119593, https://doi.org/10.1016/J.ATMOSENV.2023.119593, 2023.
Shiraiwa, M., Ammann, M., Koop, T., and Pöschl, U.: Gas uptake and chemical aging of semisolid organic aerosol particles, Proc Natl Acad Sci U S A, 108, 11003–11008, https://doi.org/10.1073/PNAS.1103045108, 2011.
Shiraiwa, M., Li, Y., Tsimpidi, A. P., Karydis, V. A., Berkemeier, T., Pandis, S. N., Lelieveld, J., Koop, T., and Pöschl, U.: Global distribution of particle phase state in atmospheric secondary organic aerosols, Nature Communications 2017 8:1, 8, 1–7, https://doi.org/10.1038/ncomms15002, 2017.

Slade, J. H., Shiraiwa, M., Arangio, A., Su, H., Pöschl, U., Wang, J., and Knopf, D. A.: Cloud droplet activation through oxidation of organic aerosol influenced by temperature and particle phase state, Geophys Res Lett, 44, 1583–1591, https://doi.org/10.1002/2016GL072424, 2017.

Song, J., Li, M., Jiang, B., Wei, S., Fan, X., and Peng, P.: Molecular Characterization of Water-Soluble Humic like Substances in Smoke Particles Emitted from Combustion of Biomass Materials and Coal Using Ultrahigh-Resolution Electrospray Ionization Fourier Transform Ion Cyclotron Resonance Mass Spectrometry, Environ Sci Technol, 52, 2575–2585, https://doi.org/10.1021/acs.est.7b06126, 2018.

Song, J., Li, M., Fan, X., Zou, C., Zhu, M., Jiang, B., Yu, Z., Jia, W., Liao, Y., and Peng, P.: Molecular Characterization of Water- And Methanol-Soluble Organic Compounds Emitted from Residential Coal Combustion Using Ultrahigh-Resolution Electrospray Ionization Fourier Transform Ion Cyclotron Resonance Mass Spectrometry, Environ Sci Technol, 53, 13607–13617, https://doi.org/10.1021/ACS.EST.9B04331, 2019.

Song, L., Chingin, K., Wang, M., Zhong, D., Chen, H., and Xu, J.: Polarity-Specific Profiling of Metabolites in Single Cells by Probe Electrophoresis Mass Spectrometry, Anal Chem, 94, 4175–4182, https://doi.org/10.1021/ACS.ANALCHEM.1C03997, 2022.

Song, L., Zhong, L., Li, T., Chen, Y., Zhang, X., Chingin, K., Zhang, N., Li, H., Hu, L., Guo, D., Chen, H., Su, R., and Xu, J.: Chemical Fingerprinting of PM2.5 via Sequential Speciation Analysis Using Electrochemical Mass Spectrometry, Environ Sci Technol, 58, https://doi.org/10.1021/ACS.EST.4C01682, 2024.

Souza, K. F., Carvalho, L. R. F., Allen, A. G., and Cardoso, A. A.: Diurnal and nocturnal measurements of PAH, nitro-PAH, and oxy-PAH compounds in atmospheric particulate matter of a sugar cane burning region, Atmos Environ, 83, 193–201, https://doi.org/10.1016/J.ATMOSENV.2013.11.007, 2014.

Tao, Y. and Murphy, J. G.: Simple Framework to Quantify the Contributions from Different Factors Influencing Aerosol pH Based on NHxPhase-Partitioning Equilibrium, Environ Sci Technol, 55, 10310–10319, https://doi.org/10.1021/ACS.EST.1C03103, 2021.

Teich, M., Van Pinxteren, D., Wang, M., Kecorius, S., Wang, Z., Müller, T., Močnik, G., and Herrmann, H.: Contributions of nitrated aromatic compounds to the light absorption of water-soluble and particulate brown carbon in different atmospheric environments in Germany and China, Atmos Chem Phys, 17, 1653–1672, https://doi.org/10.5194/ACP-17-1653-2017, 2017.

Textor, C., Schulz, M., Guibert, S., Kinne, S., Balkanski, Y., Bauer, S., Berntsen, T., Berglen, T., Boucher, O., Chin, M., Dentener, F., Diehl, T., Easter, R., Feichter, H., Fillmore, D., Ghan, S., Ginoux, P., Gong, S., Grini, A., Hendricks, J., Horowitz, L., Huang, P., Isaksen, I., Iversen, T., Kloster, S., Koch, D., Kirkevåg, A., Kristjansson, J. E., Krol, M., Lauer, A., Lamarque, J. F., Liu, X., Montanaro, V., Myhre, G., Penner, J., Pitari, G., Reddy, S., Seland, Stier, P., Takemura, T., and Tie, X.: Analysis and quantification of the diversities of aerosol life cycles within AeroCom, Atmos Chem Phys, 6, 1777–1813, https://doi.org/10.5194/ACP-6-1777-2006, 2006.

Virtanen, A., Joutsensaari, J., Koop, T., Kannosto, J., Yli-Pirilä, P., Leskinen, J., Mäkelä, J. M., Holopainen, J. K., Pöschl, U., Kulmala, M., Worsnop, D. R., and Laaksonen, A.: An amorphous solid state of biogenic secondary organic aerosol particles, Nature 2010 467:7317, 467, 824–827, https://doi.org/10.1038/nature09455, 2010.

Voliotis, A., Prokeš, R., Lammel, G., and Samara, C.: New insights on humic-like substances associated with wintertime urban aerosols from central and southern Europe: Size-resolved chemical characterization and optical properties, Atmos Environ, 166, 286–299, https://doi.org/10.1016/J.ATMOSENV.2017.07.024, 2017.

Wach, P., Spólnik, G., Surratt, J. D., Blaziak, K., Rudzinski, K. J., Lin, Y. H., Maenhaut, W., Danikiewicz, W., Claeys, M., and Szmigielski, R.: Structural Characterization of Lactone-Containing MW 212 Organosulfates

Originating from Isoprene Oxidation in Ambient Fine Aerosol, Environ Sci Technol, 54, 1415–1424, https://doi.org/10.1021/ACS.EST.9B06190, 2020.
Wang, D., Shen, Z., Zhang, Q., Lei, Y., Zhang, T., Huang, S., Sun, J., Xu, H., and Cao, J.: Winter brown carbon over six of China's megacities: Light absorption, molecular characterization, and improved source apportionment revealed by multilayer perceptron neural network, Atmos Chem Phys, 22, 14893–14904, https://doi.org/10.5194/ACP-22-14893-2022, 2022.
Wang, H., Gao, Y., Wang, S., Wu, X., Liu, Y., Li, X., Huang, D., Lou, S., Wu, Z., Guo, S., Jing, S., Li, Y., Huang, C., Tyndall, G. S., Orlando, J. J., and Zhang, X.: Atmospheric Processing of Nitrophenols and Nitrocresols From Biomass Burning Emissions, Journal of Geophysical Research: Atmospheres, 125, e2020JD033401, https://doi.org/10.1029/2020JD033401, 2020.
Wang, Y., Hu, M., Lin, P., Tan, T., Li, M., Xu, N., Zheng, J., Du, Z., Qin, Y., Wu, Y., Lu, S., Song, Y., Wu, Z., Guo, S., Zeng, L., Huang, X., and He, L.: Enhancement in Particulate Organic Nitrogen and Light Absorption of Humic-Like Substances over Tibetan Plateau Due to Long-Range Transported Biomass Burning Emissions, Environ Sci Technol, 53, 14222–14232, https://doi.org/10.1021/acs.est.9b06152, 2019.
Wang, Z. M., Zheng, M., Xie, Y. B., Li, X. X., Zeng, M., Cao, H. Bin, and Guo, L.: Molecular dynamics simulation of ozonation of p-nitrophenol at room temperature with ReaxFF force field, Wuli Huaxue Xuebao/ Acta Physico - Chimica Sinica, 33, 1399–1410, https://doi.org/10.3866/PKU.WHXB201704132, 2017.
Wu, G., Wan, X., Gao, S., Fu, P., Yin, Y., Li, G., Zhang, G., Kang, S., Ram, K., and Cong, Z.: Humic-Like Substances (HULIS) in Aerosols of Central Tibetan Plateau (Nam Co, 4730 m asl): Abundance, Light Absorption Properties, and Sources, Environ Sci Technol, 52, 7203–7211, https://doi.org/10.1021/ACS.EST.8B01251, 2018a.
Wu, Z., Wang, Y., Tan, T., Zhu, Y., Li, M., Shang, D., Wang, H., Lu, K., Guo, S., Zeng, L., and Zhang, Y.: Aerosol Liquid Water Driven by Anthropogenic Inorganic Salts: Implying Its Key Role in Haze Formation over the North China Plain, Environ Sci Technol Lett, 5, 160–166, https://doi.org/10.1021/ACS.ESTLETT.8B00021, 2018b.
Xu, H., Gu, Y., Bai, Y., Li, D., Liu, M., Wang, Z., Zhang, Q., Sun, J., and Shen, Z.: Exploration and comparison of the relationship between PAHs and ROS in PM2.5 emitted from multiple anthropogenic sources in the Guanzhong Plain, China, Science of The Total Environment, 915, 170229, https://doi.org/10.1016/J.SCITOTENV.2024.170229, 2024.
Yuan, W., Huang, R. J., Yang, L., Ni, H., Wang, T., Cao, W., Duan, J., Guo, J., Huang, H., and Hoffmann, T.: Concentrations, optical properties and sources of humic-like substances (HULIS) in fine particulate matter in Xi'an, Northwest China, Science of the Total Environment, 789, https://doi.org/10.1016/j.scitotenv.2021.147902, 2021.
Zhang, M., Cai, D., Lin, J., Liu, Z., Li, M., Wang, Y., and Chen, J.: Molecular characterization of atmospheric organic aerosols in typical megacities in China, NPJ Clim Atmos Sci, 7, 1–12, https://doi.org/10.1038/S41612-024-00784-1, 2024.
Zhao, T., Yang, L., Huang, Q., Zhang, Y., Bie, S., Li, J., Zhang, W., Duan, S., Gao, H., and Wang, W.: PM2.5-bound polycyclic aromatic hydrocarbons (PAHs) and their derivatives (nitrated-PAHs and oxygenated-PAHs) in a road tunnel located in Qingdao, China: Characteristics, sources and emission factors, Science of The Total Environment, 720, 137521, https://doi.org/10.1016/J.SCITOTENV.2020.137521, 2020.
Zou, C., Li, M., Cao, T., Zhu, M., Fan, X., Peng, S., Song, J., Jiang, B., Jia, W., Yu, C., Song, H., Yu, Z., Li, J., Zhang, G., and Peng, P.: Comparison of solid phase extraction methods for the measurement of humic-like

substances (HULIS) in atmospheric particles, Atmos Environ, 225, 117370, https://doi.org/10.1016/J.ATMOSENV.2020.117370, 2020.

Zou, C., Cao, T., Li, M., Song, J., Jiang, B., Jia, W., Li, J., Ding, X., Yu, Z., Zhang, G., and Peng, P.: Measurement report: Changes in light absorption and molecular composition of water-soluble humic-like substances during a winter haze bloom-decay process in Guangzhou, China, Atmos Chem Phys, 23, 963–979, https://doi.org/10.5194/ACP-23-963-2023, 2023.